Plant Physiol. (1985) 79, 159–164
0032-0889/85/79/0159/06/$01.00/0

Pyrophosphate-Driven Proton Transport by Microsomal Membranes of Corn Coleoptiles[1]

Received for publication November 27, 1984 and in revised form May 21, 1985

ALAIN CHANSON[2], JENNY FICHMANN, DAVID SPEAR, AND LINCOLN TAIZ*
Biology Department, Thimann Laboratories, University of California, Santa Cruz, California 95064

ABSTRACT

Corn (*Zea mays* L. cv Trojan T929) coleoptile membranes were fractionated on isopycnic sucrose density gradients. Two peaks of ATP-driven H^+-transport activity, corresponding to the previously characterized tonoplast (1.07 grams per cubic centimeter) and Golgi (1.13 grams per cubic centimeter) fractions (Chanson and Taiz, Plant Physiol 1985 78: 232–240) were localized. Coincident with these were two peaks of inorganic pyrophosphate (PPi)-driven H^+-transport. At saturating (3 millimolar) concentrations of Mg^{2+}:ATP, the rate of proton transport was further enhanced by the addition of 3 millimolar PPi, and the stimulation was additive, *i.e.* equal to the sum of the two added separately. The specific PPi analog, imidodiphosphate, antagonized PPi-driven H^+-transport, but had no effect on ATP-driven transport. Moreover, PPi-dependent proton transport in both tonoplast-enriched and Golgi-enriched fractions was strongly promoted by 50 millimolar KNO_3, unlike the ATP-dependent H^+-pumps of the same membranes. Taken together, the results indicate that PPi-driven proton transport is mediated by specific membrane-bound H^+-translocating pyrophosphatases. Both potassium and a permanent anion ($NO_3^- > Cl^-$), were required for maximum activity. The PPi-driven proton pumps were totally inhibited by *N,N'*-dicyclohexylcarbodiimide, but were insensitive to 100 millimolar vanadate. The PPi concentration in coleoptile extracts was determined using an NADH oxidation assay system coupled to purified pyrophosphate:fructose 6-phosphate 1-phosphotransferase (EC 2.7.1.90). The total pyrophosphate content of corn coleoptiles was 20 nanomoles/gram fresh weight. Assuming a cytoplasmic location, the calculated PPi concentration is sufficient to drive proton transport at 20% of the maximum rate measured *in vitro* for the tonoplast-enriched fraction, and 10% of the maximum rate for the Golgi-enriched fraction.

The role of transmembrane proton pumps as primary transport mechanisms in plant cells is now well established. The most thoroughly studied proton pumps are the H^+-translocating Mg^{2+}:ATPases, which utilize the energy of hydrolysis of Mg^{2+}:ATP to transport protons across the lipid bilayer (25). Proton-pumping Mg^{2+}:ATPases have been identified on the plasma membrane (5, 9, 18, 22, 27), tonoplast (2, 5, 6, 13, 15–17), and Golgi membranes (3, 4) in a variety of plant tissues. A Mg^{2+}:pyrophosphatase activity has also been shown to be associated with plant tonoplasts (12, 28, 30). Wagner and Mulready (28) showed that the tonoplast pyrophosphatase of *Tulipa* petals was magnesium-dependent and distinguishable from the tonoplast Mg^{2+}-ATPase. They further speculated that the tonoplast Mg^{2+}-PPase might be a proton pump, by analogy to the chromatophore pyrophosphatase of *Rhodospirillum rubrum*, which serves as a coupling factor between light-driven electron transport and PPi synthesis (1). When reconstituted into artificial proteoliposomes, the chromatophore Mg^{2+}:pyrophosphatase was capable of transporting protons using PPi as substrate (11, 12). In view of the recent reports of unexpectedly high concentrations of pyrophosphate in plant tissues (7, 24), the potential role of membrane bound pyrophosphatases as proton pumps or as coupling factors gains new significance. In this paper we report on the presence and some properties of pyrophosophate-driven proton pumps in the TEF[3] and GEF, respectively, obtained from corn coleoptile microsomal membranes. Similar findings have recently been reported by Rea and Poole (19) for beet tonoplasts. In addition, we have measured the level of PPi in coleoptile extracts.

MATERIALS AND METHODS

Plant Material. Corn (*Zea mays* L. cv Trojan T929, Pfizer-DeKalb) seeds were soaked 6 to 8 h in distilled H_2O and sown in trays with moist vermiculite, as previously described (3, 4). Seedlings were germinated in the dark at 20°C with 2 h of dim red light daily to inhibit mesocotyl growth. After 5 to 6 d, coleoptiles (~3 cm) were harvested, debladed, and collected on ice under room lights.

Membrane Isolation. Homogenization of the tissue, centrifugation of the 1,000*g* supernatant on sucrose linear and step gradients, and proton transport assays were carried out as described previously (3, 4). Briefly, coleoptiles (13 g) were chopped by hand (10 min) with razor blades in 6 ml of homogenization medium containing 250 mM sucrose, 2 mM EDTA, 1 mM DTT, 0.1% BSA, and 50 mM Tris-Mes (pH 7.8). The tissue was then ground in a mortar, strained through nylon, and the residue reground in an additional 6 ml of homogenization buffer. The combined filtrates were centrifuged at 1,000*g* (Sorvall, SS-34 rotor) and the 1 KS was collected.

The 1 KS was layered onto a linear gradient consisting of a 2-ml cushion of 45% sucrose (w/w), 20 ml 10 to 40% sucrose and 1 ml of a 10% sucrose overlay made up in gradient buffer (20 mM KCl, 1 mM DTT, 0.5 mM EDTA, and 2.5 mM Tris-Mes [pH 7.5]). The gradients were centrifuged at 80,000*g* for 3 h (Beckman L2-65B ultracentrifuge, SW 28 rotor) and fractionated into 16

[1] Supported by grant PCM-8301995 from the National Science Foundation.

[2] Recipient of a postdoctoral fellowship from the Swiss National Foundation. Permanent address: Institut de Biologie et de Physiologie Végétales, Universite de Lausanne, Bâtiment de Biologie, 1015 Lausanne, Switzerland.

[3] Abbreviations: TEF, tonoplast-enriched fraction; GEF, Golgi-enriched fraction; 1 KS, 1000*g* supernatant; BTP, bis-tris propane (1,3-bis[tris(hydroxymethyl)methylamino]propane); DCCD, *N,N'*-dicyclohexylcarbodiimide; DHAP, dihydroxyacetone phosphate; IDA, iminodiacetate; IDP, imidodiphosphate; PPase, inorganic pyrophosphatase; PFP, pyrophosphate:fructose 6-phosphate 1-phosphotransferase (EC 2.7.1.90).

fractions (1.5 ml). Alternatively, the 1 KS fraction was layered onto a step gradient consisting of a 3-ml cushion of 35% (w/w) sucrose and 5 ml each of 25, 18, and 10% sucrose in gradient buffer.

Gradient fractions were diluted to 10% sucrose with 0.5 mM EDTA, 1 mM DTT, 20 mM KCl, and 2.5 mM Tris-Mes (pH 7.5) prior to the proton transport assays. The diluted fractions were either assayed directly or frozen in liquid N_2 and stored at −70°C until use.

Proton Transport Assays. Proton transport was assayed by the quinacrine fluorescence quenching method after diluting each sample to 10% sucrose to obtain uniform osmotic conditions as previously described (4). After temperature equilibration, the reaction was initiated with either Mg^{2+}:ATP or PPi (tetrasodium salt). Because of the insolubility of Mg^{2+}:PPi in stock solutions, equimolar $MgSO_4$ was included in the transport buffer and the reaction was initiated with PPi alone. The proton gradient was collapsed by the addition of 3 μl of 1 mM monensin dissolved in ethanol (5 μM final monensin concentration) at the end of each experiment to determine the total amount of quenching. The measured activity was then multiplied by the dilution factor to obtain total activity. It should be noted that in some cases (*e.g.* Fig. 4B) this correction for dilution resulted in values of per cent total quenching in excess of 100%.

Tissue Extraction for PPi Determination. Debladed coleoptiles (4 g) were placed in a chilled mortar, quick frozen by submersion in liquid N_2, and pulverized to a fine powder with a pestle. Excess liquid N_2 was allowed to evaporate and the frozen powder was immediately transferred to a second mortar containing 8 ml of 0.45 N $HClO_4$ at room temperature (7, 24). The extraction was carried out by stirring the slurry with a glass rod for several minutes. The suspension was then centrifuged in a Sorvall RC-2B centrifuge at 27,000*g* for 15 min to remove insoluble material. The supernatant was collected, neutralized to pH 7.1 to 7.5 with 6 N KOH and placed on ice for 1 h to precipitate the perchlorate. The extract was then separated from the precipitated perchlorate by decanting, and was further clarified by centrifugation at 12,000*g* for 10 min. The final supernatant was divided into aliquots, quick frozen in liquid N_2, and stored in a −70°C freezer. Samples were assayed within 2 to 3 d, and no loss of activity was detected in samples kept frozen over a 2-week period.

Pyrophosphate Assay. Pyrophosphate was measured essentially as described by Edwards *et al.* (7). All assays were carried out at 25°C in a final volume of 1 ml. PPi concentration was determined by measuring NADH oxidation spectrophotometrically at 340 nm. In addition to either water, standard PPi solutions, or tissue extract, the assay mixture contained: 100 mM Hepes-NaOH (pH 7.5), 1 mM $MgCl_2$, 5 mM fructose-6-P, 0.15 mM NADH, 1.32 units aldolase (EC 4.1.2.13), 19.6 units triose-P isomerase (EC 5.3.1.1), 2 units glycerol-3-P dehydrogenase (EC 1.1.1.8), and 2 μM fructose-2,6-bisP. The sample containing all of the above ingredients was prepared and allowed to come to equilibrium at room temperature for 5 min. This procedure was adopted to allow background NADH oxidation caused by glycolytic intermediates present in the extract to go to completion. When a stable baseline was obtained the reaction was initiated by the addition of 0.023 units of PFP. Because of PPi contamination in one of the reagents, addition of PFP to the water control (zero PPi) resulted in a slight amount of NADH oxidation. Inclusion of 1 unit of yeast PPase (EC 3.6.1.1) in the assay mixture eliminated this reaction. Because of the PPi contamination, the absorbance change detected in the water control was routinely subtracted from the standards as well as the extract samples to obtain a true zero substrate reading.

Assays of the standard PPi solutions went to completion by 15 min. However, in all samples containing tissue extract, a slight background drift was encountered which was linear with time, was roughly proportional to the amount of sample added, was insensitive to yeast PPase, and which persisted for over 1 h. To avoid the contribution of this nonspecific drift to the total NADH oxidation, the absorbance change at 340 nm was measured after 15 min in the presence and absence of 1 unit of yeast PPase. NADH oxidation specifically due to PPi was calculated by subtracting the former from the latter. Thus, in the case of the extract, two corrections were necessary: one for nonspecific drift and the other for PPi contamination in the reaction mixture. Using the two corrections, standard curves were linear over the range of 1 to 10 nmol PPi, and NADH oxidation was stoichiometric with regard to PPi concentration (*i.e.* two NADH oxidized per PPi), similar to previously published results (7, 24). The most consistent values, as reported in this paper, were obtained with 100 μl samples. Some difficulty was experienced in obtaining proportionality to sample volumes. In general, the amount of PPi detected in the extract was proportional to the volume of extract up to 200 μl, beyond which proportionality was lost, possibly due to the presence of interfering substances. Control experiments, in which known amounts of PPi were added to the tissue prior to freezing, gave recoveries of 75%.

Chemicals. DCCD was obtained from the Aldrich Chemical Co., sodium vanadate from Fisher Scientific Co., and fructose-6-P from Calbiochem-Behring. All other chemicals and enzymes were purchased from Sigma Chemical Co.

RESULTS

Centrifugation of the 1 KS fraction of the tissue homogenate on an isopycnic linear sucrose gradient resulted in the separation of two peaks of Mg^{2+}:ATP-dependent proton transport, as measured by the quinacrine fluorescence quenching method (Fig. 1). The first peak (1.07 g/cc) was completely abolished by 50 mM KNO_3, while the second peak (1.13 g/cc) was only partially inhibited (Fig. 1). In the previous paper, evidence was presented that the first and second peaks of proton transport activity on linear isopycnic sucrose gradients correspond to the tonoplast and Golgi fractions, respectively (4). Figure 1 also shows the distribution of Mg^{2+}:PPi-dependent proton pumping across the same gradients. Two peaks of pyrophosphate-driven H^+ transport were observed, coincident with the two peaks of Mg^{2+}:ATP-dependent transport. The similarity in the profiles of the two activities suggests that proton pumping Mg^{2+}-ATPases and Mg^{2+}:pyrophosphatases are also associated with the tonoplast and Golgi membranes.

To determine whether or not the H^+-ATPase and H^+-PPase are the same enzyme, experiments were carried out with the two substrates given separately or in combination. The rationale was that if the two enzymes are identical, PPi should not stimulate any further proton pumping if ATP is present in saturating amounts. The TEF and GEF were obtained from sucrose step gradients as previously described (3, 4). Fluorescence quenching curves in the presence of 3 mM Mg^{2+}:ATP (curve a) or 3 mM Mg^{2+}:PPi (curve b) are shown in Figure 2 for the TEF (A) and GEF (B). The rate of proton transport in the presence of PPi was about 50% of the rate with ATP, and monensin rapidly collapsed the pH gradients in both cases. The concentration of ATP used was previously shown to be saturating for ATP-driven proton transport rates (see Fig. 7, Chanson and Taiz [4]). When PPi and ATP were given together, the effect was almost exactly additive (curve c), suggesting that two separate pumps were operating, although not necessarily on the same vesicle.

The effects of the pyrophosphate analog, IDP, on the ATP- and PPi-dependent activities are shown in curves d to g of Figure 2. IDP at 3 and 6 mM (curve e) had no effect on ATP-driven H^+-transport. In contrast, 3 mM IDP inhibited PPi-induced proton transport by about 50% (curve f) and 6 mM IDP was almost completely inhibitory (curve g). Similar results were ob-

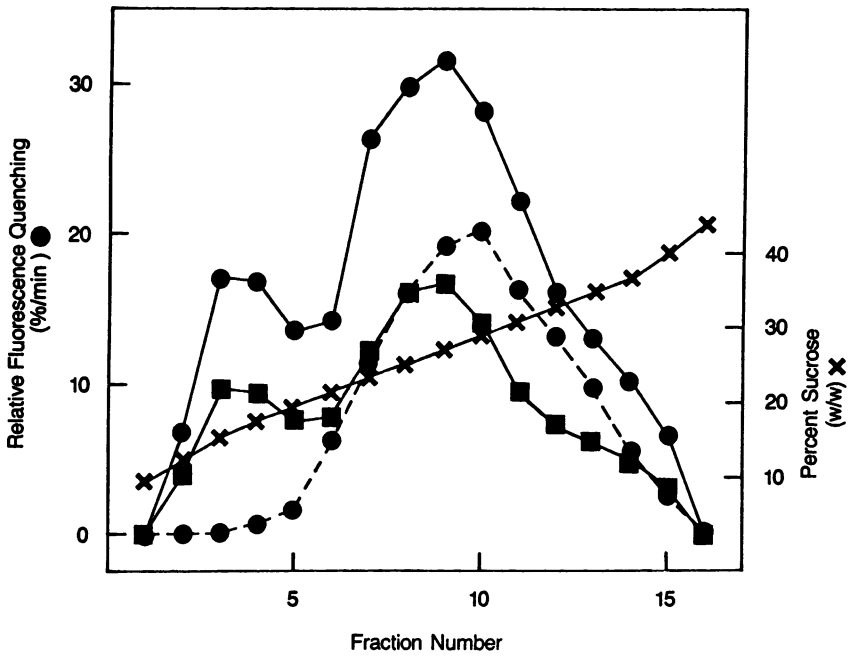

FIG. 1. Linear 10 to 40% sucrose gradient of the 1 KS centrifuged for 3 h at 80,000*g*. Relative fluorescence quenching of quinacrine in the presence of 25 mM BTP-Mes (pH 7.2), and 66 mM KCl. ATP (●——●), PPi (■——■), ATP plus 50 mM KNO_3 (●- - -●), per cent sucrose (×).

tained for both TEF and GEF. These data indicate that the H^+-ATPases and the H^+-PPases are separate enzymes.

Figure 3 illustrates the effects of various salts (50 mM) and inhibitors on PPi-dependent proton pumping in the tonoplast and Golgi fractions. All treatments, including the control, contained a background of 16 mM KCl carried over from the gradient buffer (4). Based on the initial rates, KNO_3 (curve c) was almost twice as effective as KCl (curve b) in stimulating proton transport activity. Substitution of the impermeant cation, BTP, for potassium (curve d) greatly reduced activity, as did the inclusion of the impermeant anion, IDA, in place of chloride or nitrate (curve e). These results are consistent with requirements for both potassium and a permeant anion. The greatest activity was obtained with KNO_3, in sharp contrast to the ATPases of the two fractions (4). Total activity in the presence of KNO_3 was completely inhibited by the proton channel blocker, DCCD (curve g), but was insensitive to 100 μM vanadate (curve f). No significant differences were observed in the salt or inhibitor responses of the TEF and GEF H^+-PPases.

The effect of Mg^{2+}:PPi concentration on the initial rate of H^+-pumping/mg protein is illustrated in Figure 4. In general, greater PPi-driven proton pumping was obtained in the GEF than in the TEF. An inhibition at the higher PPi concentrations was observed, which may be due to the release of inhibitory levels of free Mg^{2+} ions (Pi does not chelate Mg^{2+} as well as PPi). It was therefore not possible to calculate the K_m values of the two proton pumps. As shown in Figure 4, TEF PPi-driven proton pump activity typically occurred at a slightly lower PPi than the peak of GEF PPi-driven proton pumping. Studies with the purified enzymes are needed to determine the significance of this apparent difference.

To obtain an estimate of tissue pyrophosphate levels, PPi was determined in tissue extracts using a modification of the recently developed assay based on the reaction of PFP with PPi and fructose 6-P. The reaction is coupled to NADH oxidation via aldolase, triosephosphate isomerase and glycerol-3-P dehydrogenase (7, 24). To avoid NADH oxidation due to the presence in the extract of the glycolytic intermediates, fructose 1,6-diP, DHAP, and glyceraldehyd-3-P, all the enzymes except PFP were included in the assay buffer, and the reaction was initiated by the addition of PFP once a stable baseline was established (N. Kruger, personal communication). This procedure differs from that of the commercially available PPi assay kit in which all the enzymes are added simultaneously (24). As a further precaution against spurious sources of NADH oxidizing activity, a pyrophosphatase control was run for each sample (7). The amount of PPi in coleoptile extracts, corrected for loss, was determined to be 20 nmol g^{-1} fresh weight. It seems reasonable to assume that the majority of the PPi is located in the cytoplasm because of the high levels of soluble phosphatase and pyrophosphatase in vacuoles (12, 28). If the cytoplasm comprises ~10% of the total volume, the concentration of PPi in the cytoplasm would be about 0.2 mM. Referring to Figure 4, this PPi concentration is sufficient to drive proton transport at about 20% of the maximum rate for the TEF, and about 10% of the maximum rate for the GEF.

DISCUSSION

Two separate peaks of PPi-driven H^+-transport have been identified in linear sucrose gradients of corn coleoptile membranes. The two H^+-PPase activities coincided with the previously characterized peaks of tonoplast and Golgi ATP-driven H^+-transport (4). As in the case of ATP-dependent proton transport, quinacrine fluorescence quenching in the presence of PPi was reversed by the Na^+,K^+/H^+ ionophore, monensin, and inhibited by the proton channel blocker, DCCD. The H^+-translocating pyrophosphatases of the tonoplast and Golgi appear to be similar, but not identical. The TEF PPi-dependent proton pump was both stimulated and inhibited at lower PPi concentrations than the GEF proton pump.

Four observations suggest that the two H^+-PPase activities are distinct from the known microsomal H^+-ATPases. First, PPi and ATP are additive in their effects on proton transport, even at saturating substrate concentrations. Second, PPi-driven proton transport is specifically blocked by the pyrophosphate analog, IDP. Third, PPi-driven H^+-transport is strongly promoted by 50 mM KNO_3, whereas the same concentration of KNO_3 inhibits the ATP-driven proton pumps of the tonoplast by 100% (2, 6, 16, 17, 28) and Golgi by 50% (4). Fourth, unlike the plasma membrane H^+-ATPase (4, 5, 9, 18, 21), the H^+-PPases of the tonoplast and Golgi are insensitive to 100 μM vanadate. Although the results indicate that the ATPases and pyrophosphatases are

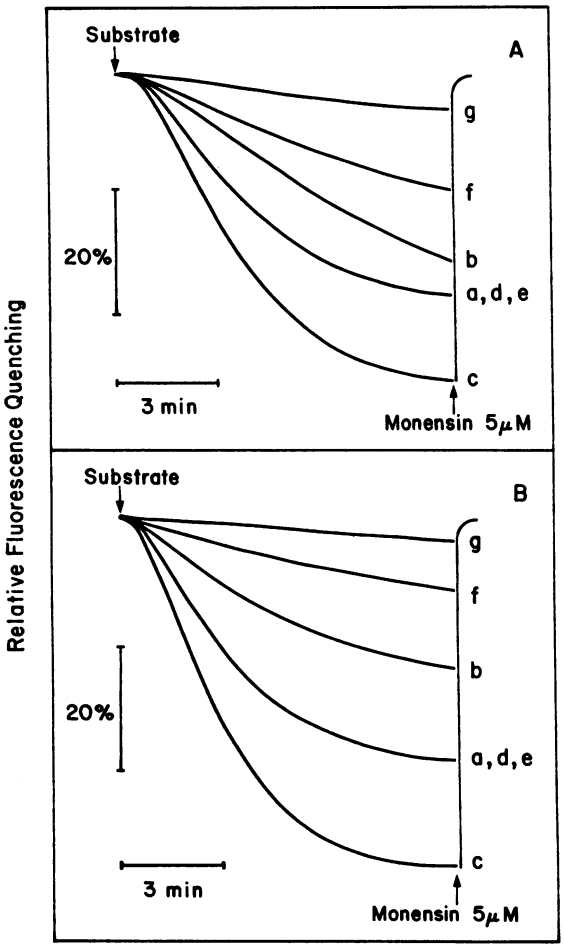

FIG. 2. Quinacrine fluorescence quenching in the presence of 66 mM KCl. Fractions were obtained from a sucrose step gradient and diluted to 10% sucrose. The traces shown are uncorrected for the dilution factor. A, 10 to 18% (tonoplast-enriched fraction); B, 25 to 35% (Golgi-enriched fraction). Curve a, 3 mM ATP, 3 mM $MgSO_4$; b, 3 mM PPi, 3 mM $MgSO_4$; c, 3 mM ATP, 3 mM PPi, 6 mM $MgSO_4$; d, 3 mM ATP, 3 mM $MgSO_4$, 3 mM IDP; e, 3 mM ATP, 3 mM $MgSO_4$, 6 mM IDP; f, 3 mM PPi, 3 mM $MgSO_4$, 3 mM IDP; g, 3 mM PPi, 3 mM $MgSO_4$, 6 mM IDP.

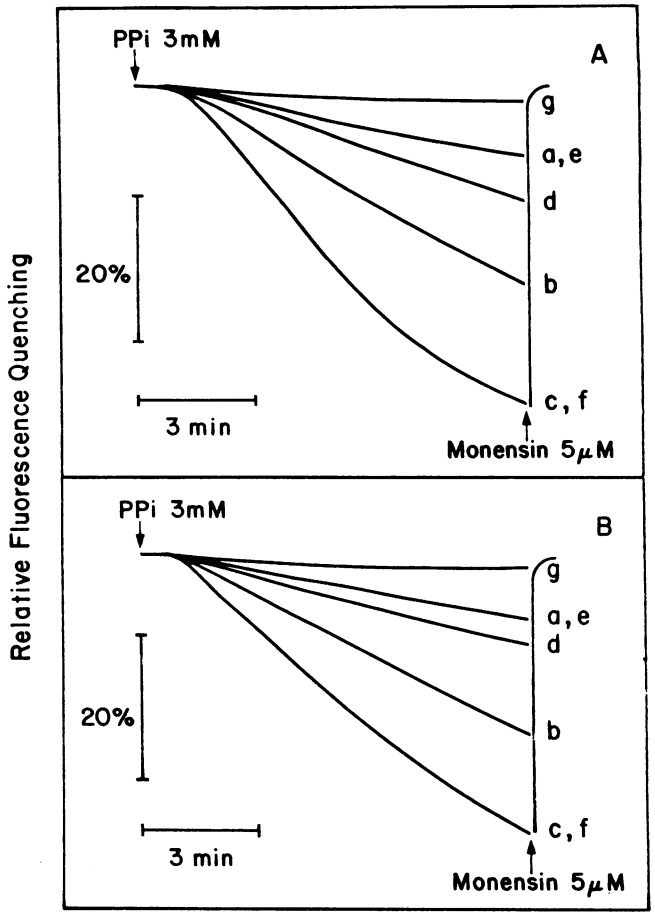

FIG. 3. Effects of different salts and inhibitors on PPi-dependent proton transport in the presence of 3 mM $MgSO_4$. Fractions were obtained from a sucrose step gradient and diluted to 10% sucrose. A, 10 to 18% (w/w) (tonoplast-enriched fraction); B, 25 to 35% (Golgi-enriched fraction). Curve a, Control, 16 mM KCl; b, plus 50 mM KCl; c, plus 50 mM KNO_3; d, plus 50 mM BTP-Cl; e, plus 50 mM KIDA; f, plus 50 mM KNO_3 and 100 μM vanadate; g, plus 50 mM KNO_3 and 100 μM DCCD (in 1% ethanol).

separate enzymes, it does not necessarily follow that they are present on the same membrane vesicles. It is possible that two separate populations of tonoplast vesicles and Golgi cisternae are responsible for the two transport activities.

Pyrophosphatase activity has previously been shown to be associated with microsomal (10) and vacuolar membranes (12, 28–30). Walker and Leigh (30) were the first to suggest that the tonoplast PPase was a proton pump. Churchill and Sze (6) reported surprisingly high PPi-induced proton transport by microsomal membranes of oat roots, although the relationship to the H^+-ATPase was not explored. After this paper was submitted a report appeared by Rea and Poole (19) demonstrating PPi-driven proton transport in beet root tonoplasts. They also concluded that ATPase and PPase are different enzymes. Our results thus confirm and extend those of Churchill and Sze (6) and Rea and Poole (19). Unlike the results of Rea and Poole (19), however, PPi-dependent proton pumping by corn coleoptile membranes was stimulated by nitrate rather than inhibited. This is consistent with the previously reported nitrate stimulation of PPase activity in beet membranes (19, 30).

Evidence has been presented that *Rhodospirilum* chromatophores (1, 11, 22) and beef heart mitochondria (14) contain coupling factor pyrophosphatases which synthesize PPi during electron transport. When these coupling factor pyrophosphatases were solubilized and reconstituted into proteoliposomes they pumped protons in response to exogenous PPi (11, 14, 23). Although we are not aware of any reports of pyrophosphatase in plant mitochondria, the question arises whether any of the PPi-dependent proton transport activity measured in this study could be derived from mitochondrial membranes. Although a mitochondrial origin cannot be ruled out, the mitochondrial marker, Cyt *c* oxidase, is well-separated from both the ATP- and PPi-dependent H^+-pumping peaks on sucrose gradients (4; A. Chanson, L. Taiz, unpublished data).

ATP is generally regarded as the principal energy source for proton transport across plant cell membranes (25), although there are recent reports of plasma membrane proton pumps driven by redox reactions involving NADH or NADPH (20, and references therein). The steady state concentration of cytoplasmic PPi has been assumed, until recently, to be maintained at extremely low levels, inasmuch as many cellular anabolic reactions which generate PPi as a byproduct, *e.g.* amino acid acylation or the synthesis of UDPG, are apparently made thermodynamically favorable and irreversible by the continuous removal of PPi (26). If the lowering of PPi levels were mediated by a soluble inorganic pyrophosphatase, as is often stated in texts (*e.g.* 26), and the

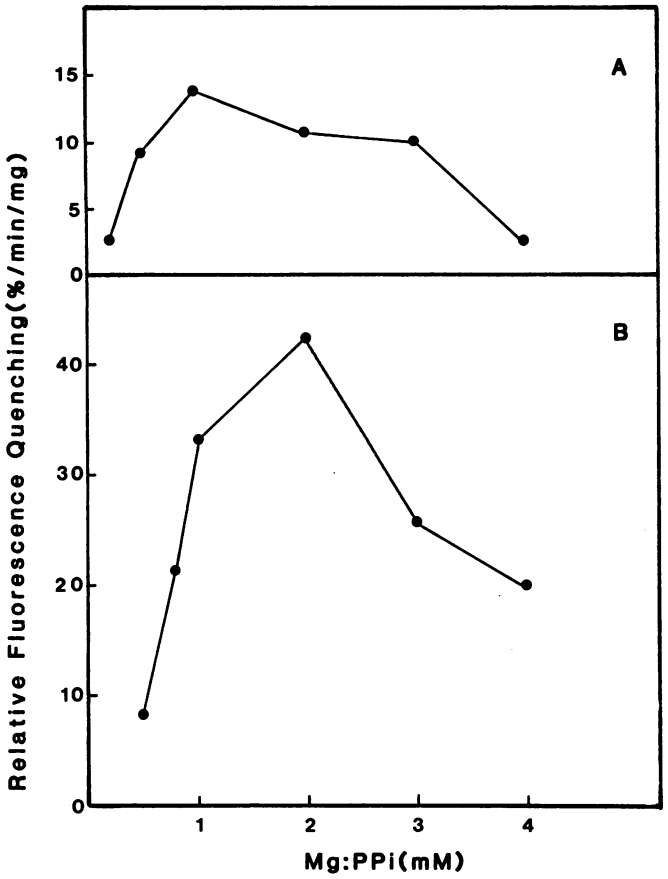

FIG. 4. Effect of Mg^{2+}:PPi concentration on proton transport as measured by quinacrine fluorescence quenching in the presence of 50 mM KNO_3. Fractions were obtained from a sucrose step gradient. A, 10 to 18% (tonoplast-enriched fraction); B, 25 to 35% (Golgi-enriched fraction). Both fractions were diluted to 10% sucrose for uniform osmotic conditions. The rates shown were multiplied by the appropriate dilution factor for the TEF (1.27) and GEF (2.97).

reaction proceeded very far towards equilibrium, it has been estimated for liver cells that the cytoplasmic PPi concentration would be about 10 nM, given an intracellular Pi concentration of 4 mM (8). Cytoplasmic Pi in plant cells has recently been determined to be about 5 to 6 mM using P^{31}-NMR (20), comparable to the level in liver cells. The measured PPi in liver cells is 2 to 3 orders of magnitude higher than the predicted value based on an energy-wasting hydrolysis reaction (8), while the measured PPi levels in plants presented here and in previous papers (7, 24) are 3 to 4 orders of magnitude higher. This suggests either that: (a) PPi is removed by sequestration into a separate compartment, or (b) PPi removal is coupled to one or more energy-conserving reactions (7, 24).

In liver, PPi is apparently not compartmentalized. This was demonstrated by measuring the concentrations of UTP, glucose 1-P, and UDPG, which should be in equilibrium with PPi via the cytosolic enzyme, UDPG-pyrophosphorylase, if PPi is in the cytosol (8). The actual measured concentration of PPi in liver was similar to the predicted level based on the equilibrium constant of UDPG-pyrophosphorylase. Similar studies are needed for plant tissues. However, assuming that PPi is in the cytosol, the concentration (0.2 mM), while much higher than predicted for equilibria with soluble PPases (10 nM [8]), is still marginal for driving proton transport (see Fig. 4), at least for the Golgi-enriched fraction. It is possible that membrane H^+-PPase activity is normally enhanced *in vivo* by an activator molecule. Alternatively, the pyrophosphatases may, in the presence of steep proton gradients and low cytoplasmic PPi concentrations, couple proton transport in the reverse direction to PPi synthesis, similar to the coupling factor PPase of *Rhodospirillum rubrum* and beef liver mitochondria (1, 11, 14, 23). This would effectively dissipate excessive ATP-generated pH gradients across cellular membranes in an energy-conserving step. Implicit in this model is the requirement that the two pumps be located on the same membrane. Perhaps when cytoplasmic PPi levels are relatively high, as might be expected in young, rapidly growing tissues with high rates of biosynthesis, membrane-bound pyrophosphatases might utilize the energy of hydrolysis of PPi to drive proton transport into the vacuole and Golgi cisternae. This would alleviate competition for ATP between biosynthetic reactions and membrane transport processes. The hydrolysis of PPi would, in turn, help to maintain favorable conditions in the cytoplasm for rapid biosynthesis. When cytoplasmic PPi concentrations are at a minimum due to low biosynthetic rates, *e.g.* in mature tissues, the reverse reaction might occur, *i.e.* PPi synthesis might be driven by the transmembrane pH gradient. This would ensure that PPi levels did not fall below a critical level for other PPi-requiring reactions (7, 24). In this way rates of biosynthetic reactions might be coupled to the reversible transport of protons across these membranes.

Acknowledgments—We thank the Pfizer-DeKalb Company for their generous supply of the Trojan T929 corn seeds. We also thank Dr. Suzanne Mandala for helpful discussions throughout this study and for a critical review of the manuscript.

LITERATURE CITED

1. BALTSCHEFFSKY M, H BALTSCHEFFSKY, L-V VON STEDINGK 1966 Light-induced energy conversion and the inorganic pyrophosphatase reaction in chromatophores from *Rhodospirillum rubrum*. Brookhaven Symp Biol 19: 246–257
2. BENNETT AB, SD O'NEILL, RM SPANSWICK 1984 H^+-ATPase activity from storage tissue of *Beta vulgaris*. I. Identification and characteristics of an anion-sensitive H^+-ATPase. Plant Physiol 74: 538–544
3. CHANSON A, E MCNAUGHTON, L TAIZ 1984 Evidence for a KCl-stimulated Mg^{2+}-ATPase on the Golgi of corn coleoptiles. Plant Physiol 76: 498–507
4. CHANSON A, L TAIZ 1985 Evidence for an ATP-dependent proton pump on the Golgi of corn coleoptiles. Plant Physiol 78: 232–240
5. CHURCHILL KA, B HOLAWAY, H SZE 1983 Separation of two types of electrogenic H^+-ATPases from oat roots. Plant Physiol 73: 921–928
6. CHURCHILL KA, H SZE 1983 Anion-sensitive, H^+-pumping ATPase in membrane vesicles from oat roots. Plant Physiol 71: 610–617
7. EDWARDS J, T AP REES, PM WILSON, S MORRELL 1984 Measurement of the inorganic pyrophosphate in tissues of *Pisum sativum* L. Planta 162: 188–191
8. GUYNN RW, D VELOSCO, JR RANDOLPH LAWSON, RL VEECH 1974 The concentration and control of cytoplasmic free inorganic pyrophosphate in rat liver *in vivo*. Biochem J 140: 369–375
9. IMBRIE CW, TM MURPHY 1984 Solubilization and partial purification of ATPase from a rose cell plasma membrane fraction. Plant Physiol 74: 611–616
10. KARLSSON J 1975 Membrane-bound potassium and magnesium ion-stimulated inorganic pyrophosphatase from roots and cotyledons of sugar beet (*Beta vulgaris* L.). Biochem J 178: 539–547
11. KONDRASHIN AA, VG REMENNIKOV, VD SAMUILOV, VP SKULACHEV 1980 Reconstitution of biological molecular generators of electric current. Inorganic pyrophosphatase. Eur J Biochem 113: 219–222
12. LEIGH RA, RR WALKER 1980 ATPase and acid phosphatase activities associated with vacuoles isolated from storage roots of red beet (*Beta vulgaris* L.). Planta 150: 222–229
13. MANDALA S, IJ METTLER, L TAIZ 1982 Localization of the proton pump of corn coleoptile microsomal membranes by density gradient centrifugation. Plant Physiol 70: 1743–1747
14. MANSUROVA SE, YA SHAKHOV, IS KULAEV 1977 Mitochondrial pyrophosphatase is a coupling factor of respiration and pyrophosphate synthesis. FEBS Lett 74: 31–34
15. MARIN B 1983 Evidence for an electrogenic adenosine-triphosphatase in *Hevea* tonoplast vesicles. Planta 157: 324–330
16. METTLER IJ, S MANDALA, L TAIZ 1982 Characterization of *in vitro* proton pumping by microsomal vesicles isolated from corn coleoptiles. Plant Physiol 70: 1738–1742
17. O'NEILL SD, AB BENNETT, RM SPANSWICK 1983 Characterization of a NO_3^--sensitive H^+-ATPase from corn roots. Plant Physiol 72: 837–846
18. O'NEILL SD, RM SPANSWICK 1984 Characterization of native and reconstituted plasma membrane H^+-ATPase from the plasma membrane of *Beta*

vulgaris. J Membr Biol 79: 245–256
19. REA PA, RJ POOLE 1985 Proton-translocating inorganic pyrophosphatase in red beet (*Beta vulgaris* L.) tonoplast vesicles. Plant Physiol 77: 46–52
20. REBEILLE F, R BLIGNY, R DOUCE 1984 Is the cytosolic Pi concentration a limiting factor for plant cell respiration? Plant Physiol 74: 355–359
21. RUBINSTEIN B, AI STERN, RG STOUT 1984 Redox activity at the surface of oat root cells. Plant Physiol 76: 386–391
22. SCHERER GFE 1984 Subcellular localization of H^+-ATPase from pumpkin hypocotyls (*Cucurbita maxima* L.) by membrane fractionation. Planta 160: 348–356
23. SHAKHOV YA, P NYREN, M BALTSCHEFFSKY 1982 Reconstitution of highly purified proton-translocating pyrophosphatase from *Rhodospirillum rubrum*. FEBS Lett 146: 177–180
24. SMYTH DA, CC BLACK 1984 Measurement of the pyrophosphate content of plant tissues. Plant Physiol 75: 862–864
25. SPANSWICK RM 1981 Electrogenic ion pumps. Annu Rev Plant Physiol 32: 267–289
26. STRYER L 1981 Biochemistry, Ed 2. WH Freeman, San Francisco.
27. VARA F, R SERRANO 1982 Partial purification and properties of the proton-translocating ATPase of plant plasma membranes. J Biol Chem 257: 12826–12830
28. WAGNER GJ, P MULREADY 1983 Characterization and solubilization of nucleotide-specific Mg^{2+}-ATPase and Mg^{2+}-pyrophosphatase of tonoplast. Biochim Biophys Acta 728: 267–280
29. WALKER RR, RA LEIGH 1981 Characterization of a salt-stimulated ATPase activity associated with vacuoles isolated from storage roots of red beet (*Beta vulgaris* L.). Planta 153: 140–149
30. WALKER RR, RA LEIGH 1981 Mg^{2+}-dependent, cation-stimulated inorganic pyrophosphatase associated with vacuoles isolated from storage roots of red beet (*Beta vulgaris* L.). Planta 153: 150–155